Supplementary Materials

Lorenzo Nava[1, 2], Maximilian Van Wyk de Vries[2, 1], and Louie Elliot Bell[2, 3]

[1]Department of Earth Sciences, University of Cambridge, Cambridge, UK
[2]Department of Geography, University of Cambridge, Cambridge, UK
[3]Scott Polar Research Institute, University of Cambridge, Cambridge, UK

Correspondence: Lorenzo Nava (ln413@cam.ac.uk)

S1 Subpixel Peak Refinement Methods

To achieve subpixel precision in displacement estimation from correlation surfaces, we implemented and evaluated several widely used interpolation methods, as described below.

Center of Mass Interpolation

The center of mass method estimates the subpixel displacement by computing the intensity-weighted centroid of a local correlation window around the integer peak.

Given a peak at location (i, j) in the correlation surface, we extract a 3×3 window centered at the peak:

$$\texttt{local\_window} = C[i-1:i+2, j-1:j+2]$$

where C is the correlation surface. The subpixel offsets $(\delta x, \delta y)$ are calculated using the center of mass:

$$(\delta y, \delta x) = \texttt{center\_of\_mass}(\texttt{local\_window})$$

The final subpixel displacement relative to the search window is:

$$dx = \delta x + (j-1) - \frac{b_s}{2}$$
$$dy = \delta y + (i-1) - \frac{b_s}{2}$$

where b_s is the block size of the search window.

This method assumes the correlation peak is unimodal and symmetric. It is efficient but less accurate in the presence of noise or multiple local maxima.

S1.1 Parabolic Interpolation

This method fits a quadratic curve to three consecutive values along each axis of the correlation surface (i.e., the peak and its immediate neighbors). The subpixel offset is computed as the location of the parabola's vertex:

$$\delta = \frac{1}{2} \cdot \frac{f_{-1} - f_{+1}}{f_{-1} - 2f_0 + f_{+1}}$$

where f_{-1}, f_0, and f_{+1} are the correlation values at the neighboring and central pixels. This offset is added to the integer peak position to refine the displacement estimate.

S1.2 Gaussian Interpolation

Gaussian interpolation assumes the correlation peak follows a Gaussian profile in log space. A log-parabola is fit to the peak and its neighbors:

$$\delta = \frac{\log(f_{-1}) - \log(f_{+1})}{2 \cdot (\log(f_{-1}) - 2\log(f_0) + \log(f_{+1}))}$$

The result is clamped to the range $[-1, 1]$ to avoid instabilities in noisy regions.

S1.3 Offset Smoothing (OS) Methods: OS3, OS5, OS7

These methods compute a weighted centroid over a fixed-size window (3×3, 5×5, or 7×7) centered on the correlation peak:

- The average value of all non-central pixels is subtracted from the window to suppress the background.
- Negative weights are discarded, and the remainder is normalized.
- The weighted centroid is computed using a meshgrid of pixel offsets.

This approach improves robustness in low-contrast or noisy correlation peaks and captures off-center maxima.

Intensity Peak Gradient (IPG) Method

The Intensity Peak Gradient (IPG) method estimates subpixel displacements by fitting a second-order surface (a local quadratic model) to the correlation peak using image gradients and curvature. It is mathematically equivalent to a second-order Taylor expansion around the peak (Liu et al., 2021; Guizar-Sicairos et al., 2008).

- First-order partial derivatives f_x, f_y, and second-order derivatives f_{xx}, f_{yy}, and f_{xy} are estimated using finite differences over a 3×3 window.

– The correlation surface $f(\boldsymbol{x})$ is locally approximated as:

$$f(\boldsymbol{x}+\delta\boldsymbol{x}) \approx f(\boldsymbol{x}) + \nabla f^\top \delta\boldsymbol{x} + \frac{1}{2}\delta\boldsymbol{x}^\top H \delta\boldsymbol{x}$$

where $\nabla f = [f_x, f_y]^\top$ is the gradient vector and H is the Hessian matrix:

$$H = \begin{bmatrix} f_{xx} & f_{xy} \\ f_{xy} & f_{yy} \end{bmatrix}$$

– The subpixel offset $\delta\boldsymbol{x}$ is obtained by solving:

$$\delta\boldsymbol{x} = -H^{-1}\nabla f$$

– To ensure robustness, the method includes checks on the Hessian condition number and limits on displacement magnitude to avoid unstable or spurious estimates.

S2 Subpixel Methods Comparison

To validate the subpixel refinement accuracy and estimate potential biases, we introduced synthetic, uniform subpixel shifts in both the north–south (NS) and east–west (EW) directions. These shifts were applied in a step-wise pattern every 200 pixels across the image. EW shifts ranged from +0.1 to +1 pixels, while NS shifts ranged from –0.1 to –1 pixels (Zheng et al., 2023). All the test are executed on a machine equipped with an Intel(R) Xeon(R) w3-2423 CPU and 60 GB of RAM.

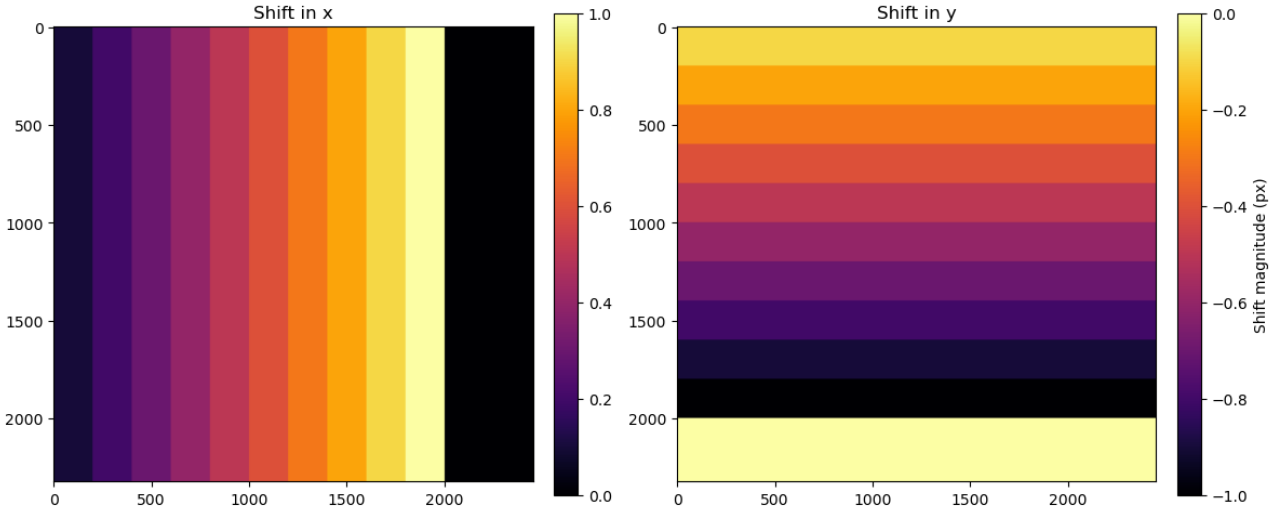

Figure S1. Synthetic subpixel shift used in the comparison.

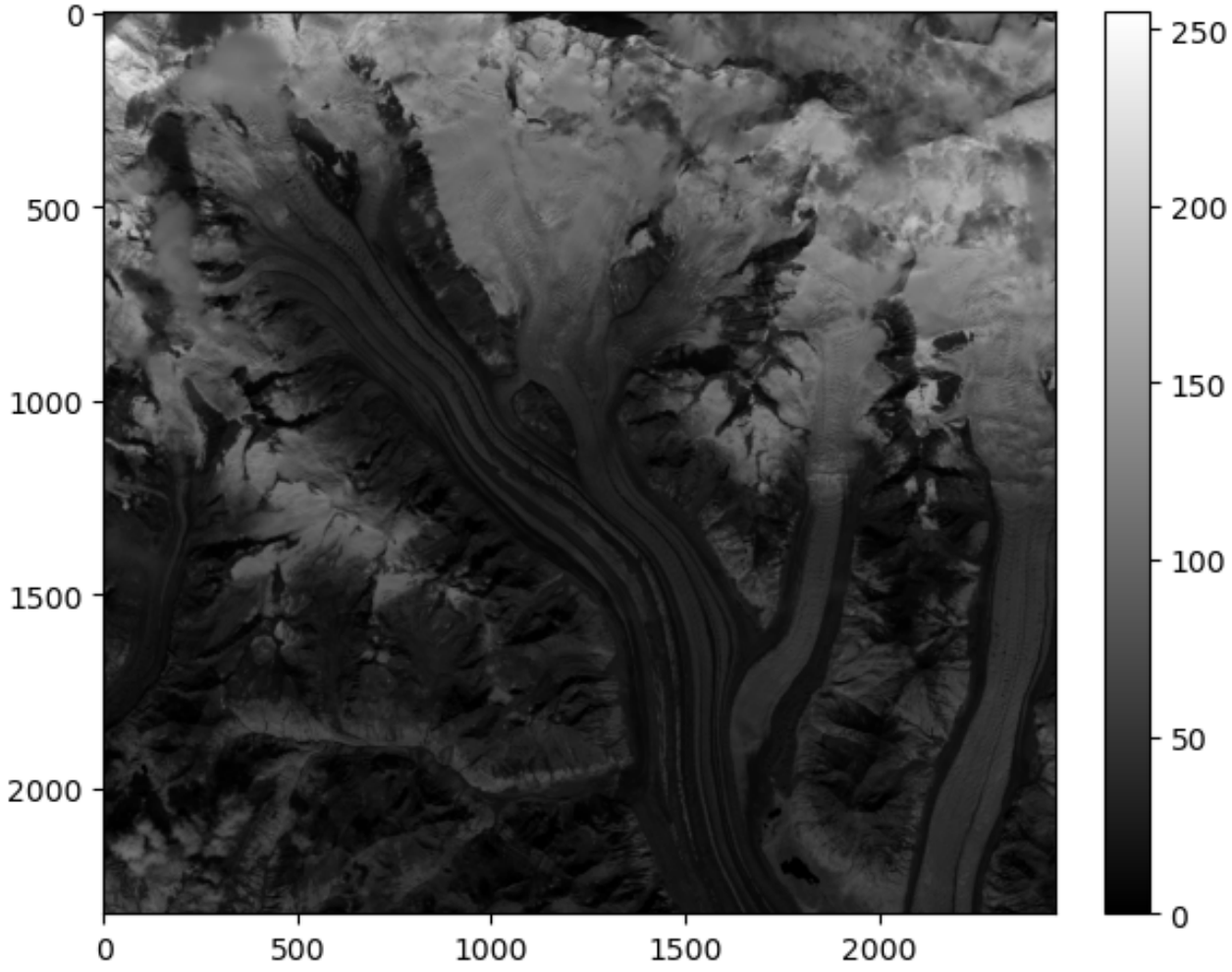

Figure S2. Original Sentinel-2 image used in the comparison.

We then ran the feature tracking algorithm with Phase Cross Correlation PCC and Normalised Cross Correlation $\mathrm{NCC_{FFT}}$ and the 7 subpixel strategies implemented subpixel and compared the retrieved displacements to the known, applied shifts. This allowed us to quantify the accuracy, precision, and potential directional bias of the subpixel estimation under ideal, noise-free conditions.

S2.1 $\mathbf{NCC_{FFT}}$

$\mathrm{NCC_{FFT}}$ accelerates the computation of the conventional NCC in spatial domain by leveraging the convolution theorem. Given a reference chip $R(x, y)$ and a target chip $T(x + u, y + v)$ at a displacement (u, v) the cross-correlation is computed in the frequency domain as:

$$\mathrm{NCC}_{\mathrm{FFT}}(u,v) = \mathcal{F}^{-1}\left(\frac{\mathcal{F}(R)\cdot\mathcal{F}(T)^{*}}{|\mathcal{F}(R)\cdot\mathcal{F}(T)^{*}|+\epsilon}\right) \tag{1}$$

Here, $\mathcal{F}$ denotes the Fourier transform, * is the complex conjugate, and ϵ is a small constant added for numerical stability. The inverse Fourier transform $\mathcal{F}^{-1}$ returns the cross-correlation surface, where the peak corresponds to the best match.

Table S1. $\mathrm{NCC}_{\mathrm{FFT}}$ subpixel refinement: bias, NMAD, and per-block runtimes

Method	Bias_x	Bias_y	NMAD_x	NMAD_y	Runtime per block (s)
center of mass	-0.03016	0.00867	0.13743	0.12744	7.55×10^{-5}
parabolic	-0.02899	0.00288	0.11450	0.14476	5.40×10^{-5}
gaussian	-0.17120	0.19141	0.31677	0.60960	7.70×10^{-5}
os3	-0.11807	0.00201	0.14583	0.11762	1.39×10^{-4}
os5	-0.12663	0.03664	0.16526	0.09148	1.28×10^{-4}
os7	-0.20461	0.13346	0.24607	0.20012	1.14×10^{-4}
ipg	-0.16572	0.18519	0.32336	0.29196	8.58×10^{-5}
ensemble	-0.21329	0.19178	0.32542	0.30844	1.68×10^{-4}

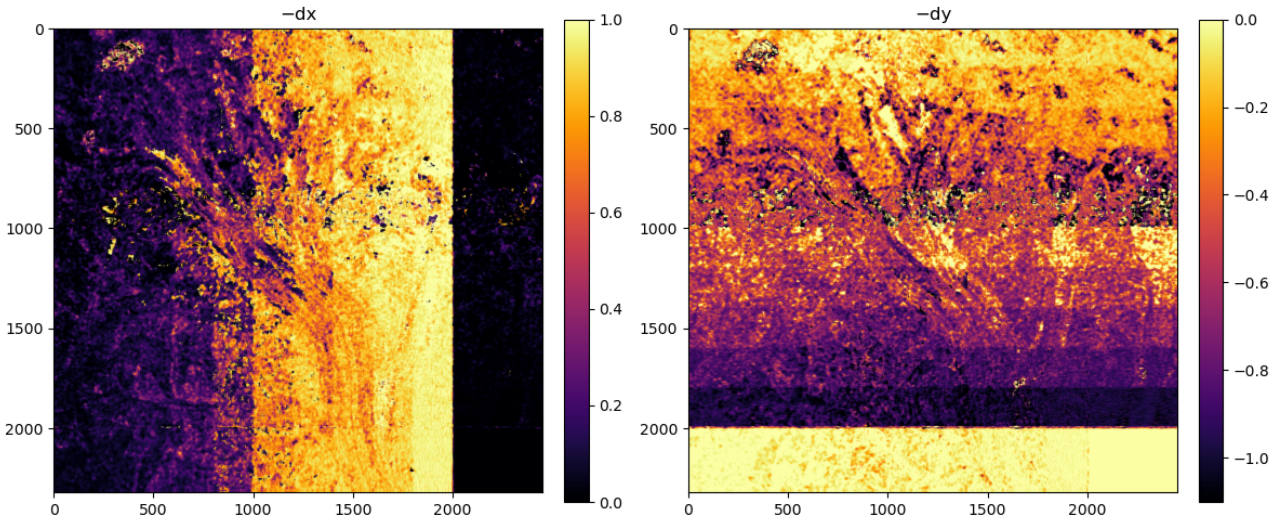

Figure S3. $\mathrm{NCC}_{\mathrm{FFT}}$ center of mass subpixel refinement estimates.

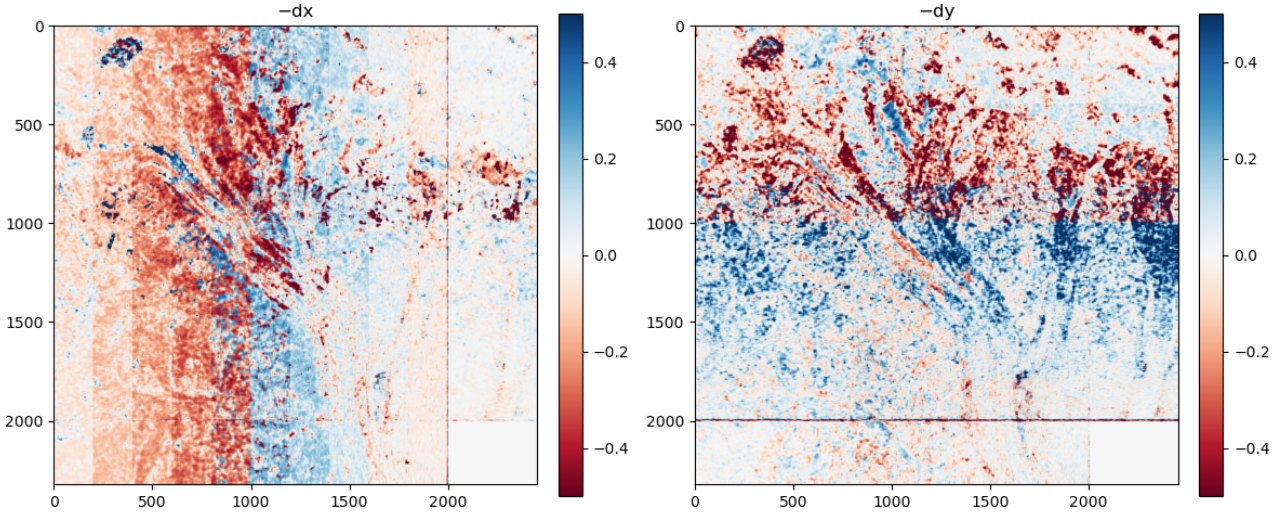

Figure S4. $\mathrm{NCC}_{\mathrm{FFT}}$ center of mass subpixel refinement residuals.

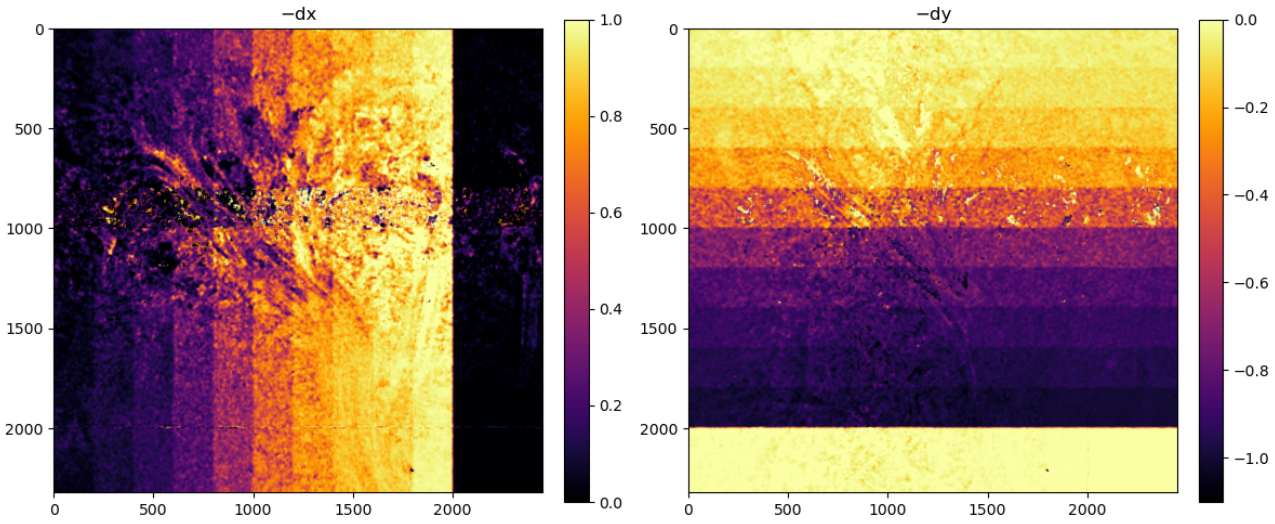

Figure S5. $\mathrm{NCC}_{\mathrm{FFT}}$ parabolic subpixel refinement estimates.

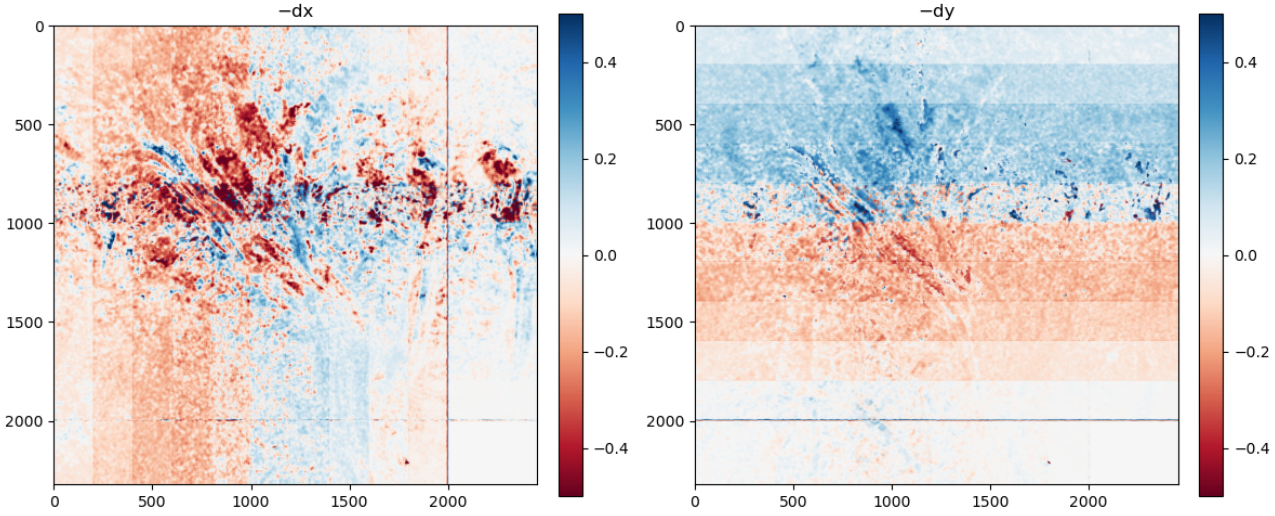

Figure S6. $\mathrm{NCC}_{\mathrm{FFT}}$ parabolic subpixel refinement residuals.

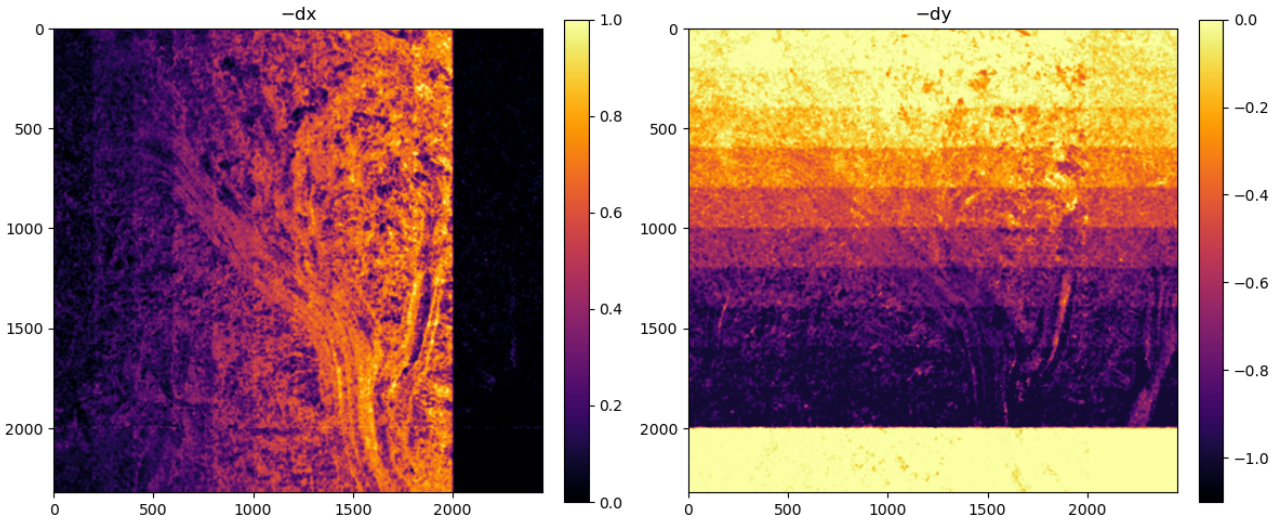

Figure S7. $\mathrm{NCC}_{\mathrm{FFT}}$ os3 subpixel refinement estimates.

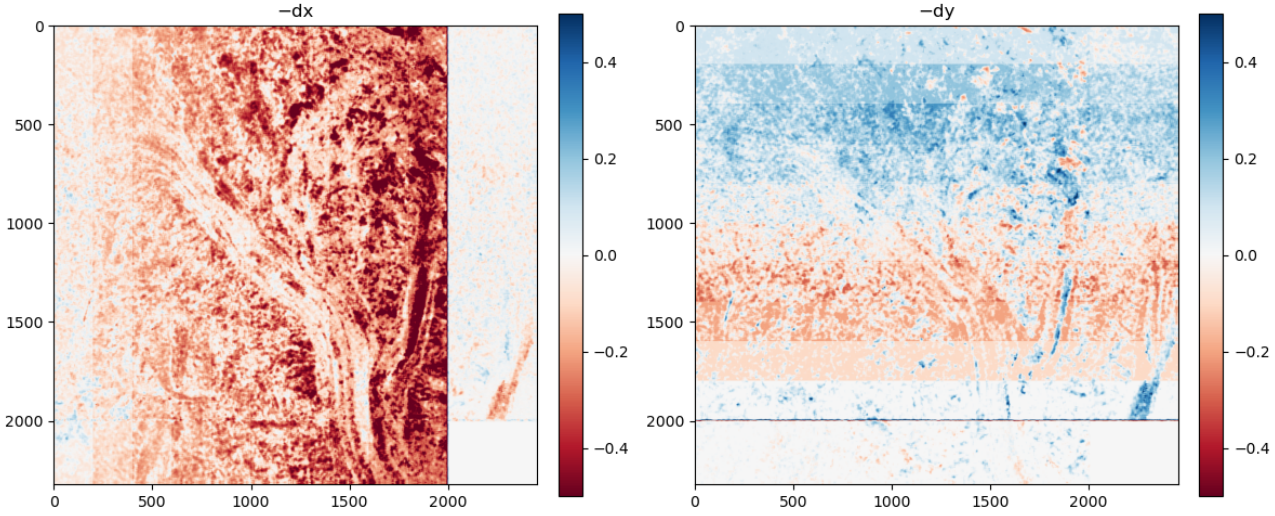

Figure S8. $\mathrm{NCC}_{\mathrm{FFT}}$ os3 subpixel refinement residuals.

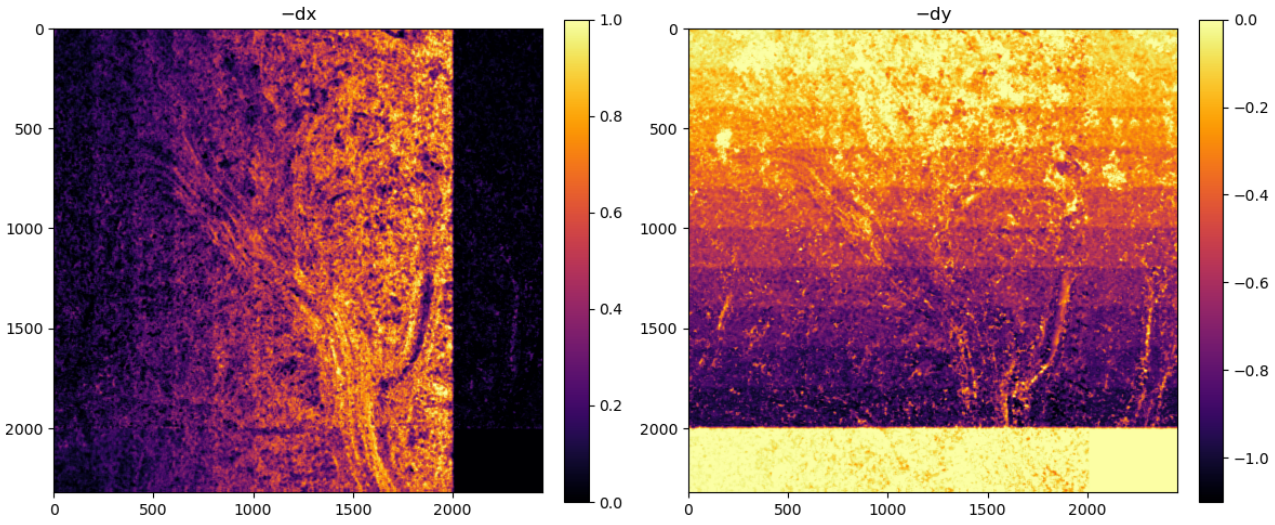

Figure S9. $\mathrm{NCC}_{\mathrm{FFT}}$ os5 subpixel refinement estimates.

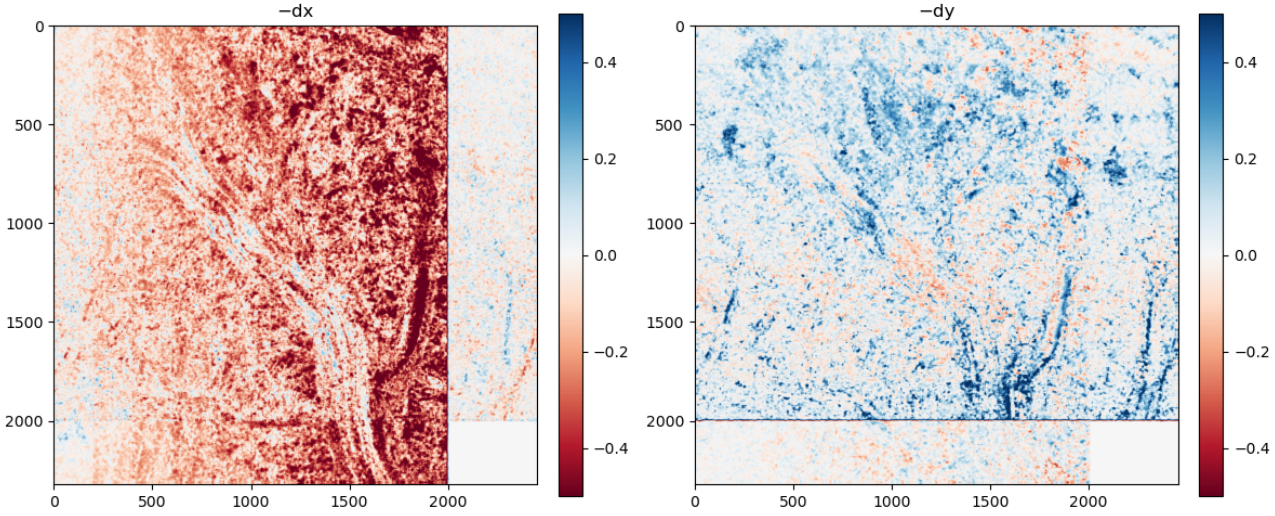

Figure S10. $\mathrm{NCC}_{\mathrm{FFT}}$ os5 subpixel refinement residuals.

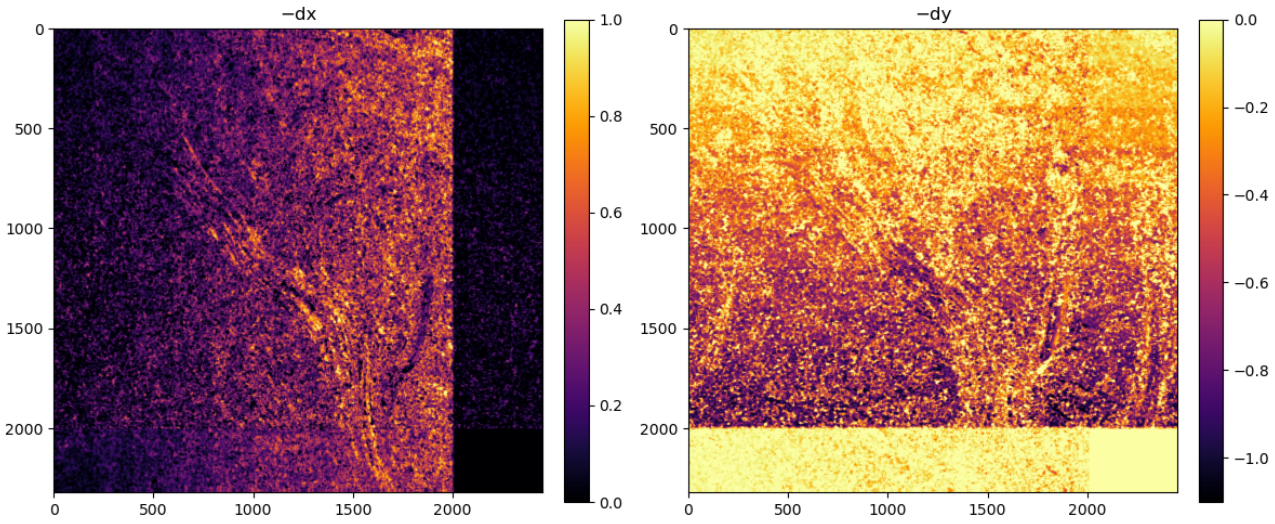

Figure S11. $\mathrm{NCC}_{\mathrm{FFT}}$ os7 subpixel refinement estimates.

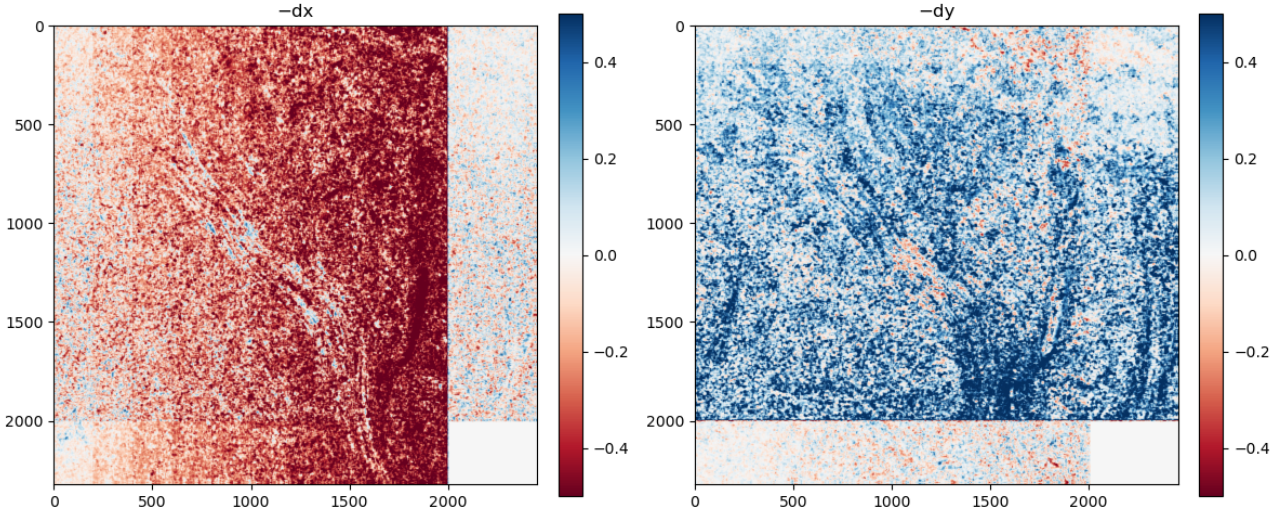

Figure S12. $\mathrm{NCC}_{\mathrm{FFT}}$ os7 subpixel refinement residuals.

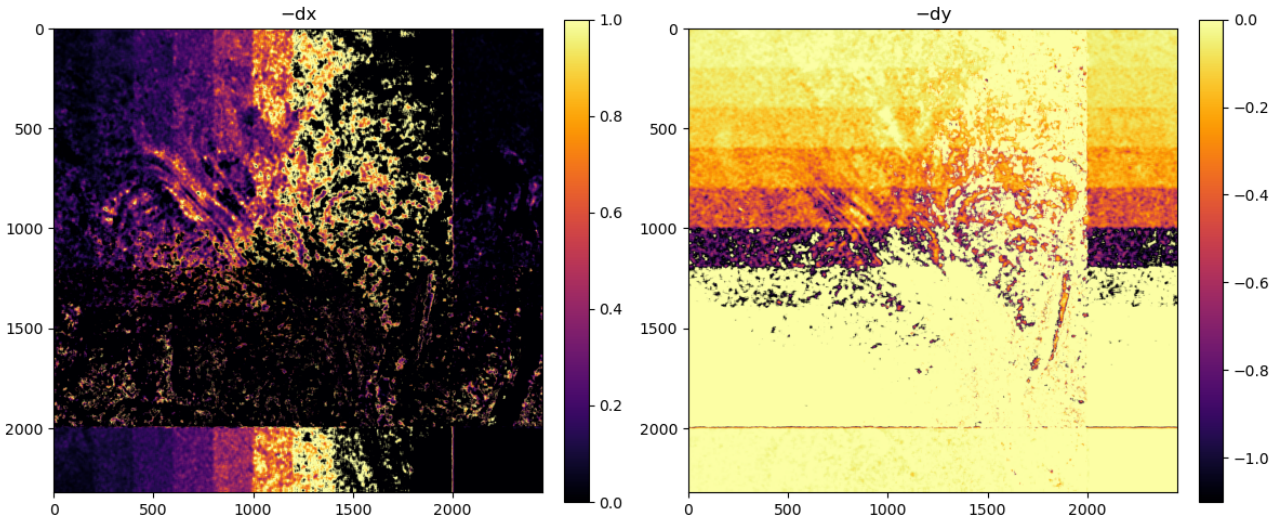

Figure S13. $\mathrm{NCC}_{\mathrm{FFT}}$ ipg subpixel refinement estimates.

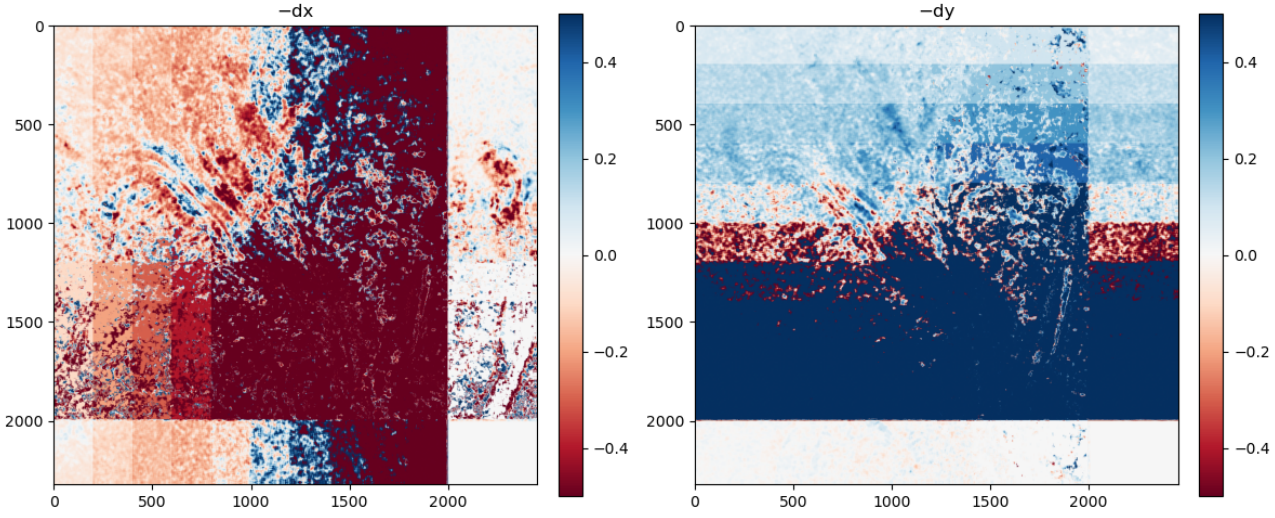

Figure S14. $\mathrm{NCC}_{\mathrm{FFT}}$ ipg subpixel refinement residuals.

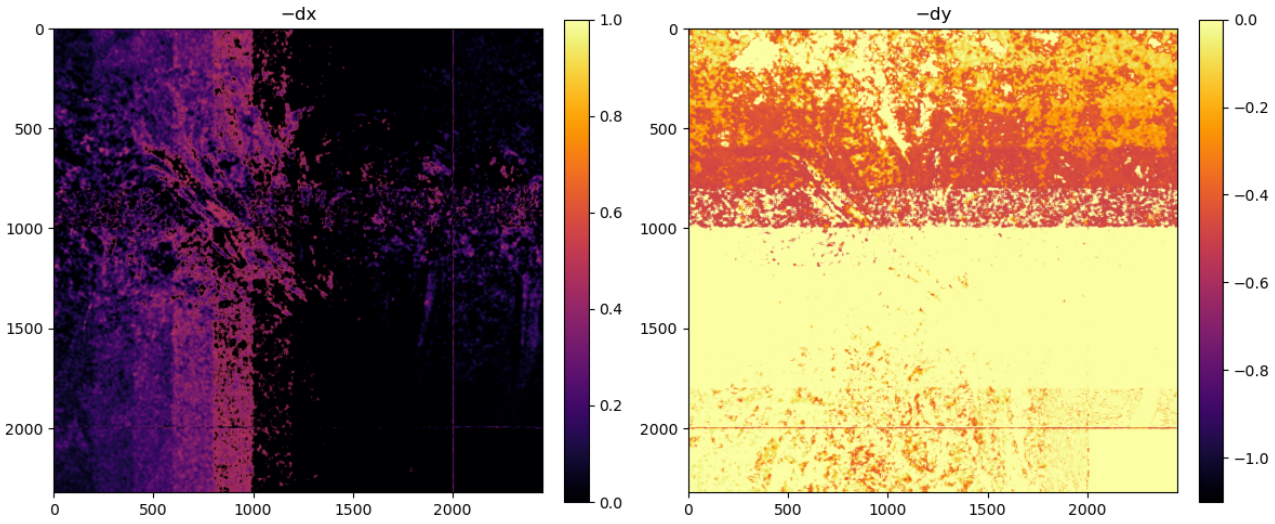

Figure S15. $\mathrm{NCC}_{\mathrm{FFT}}$ gaussian subpixel refinement estimates.

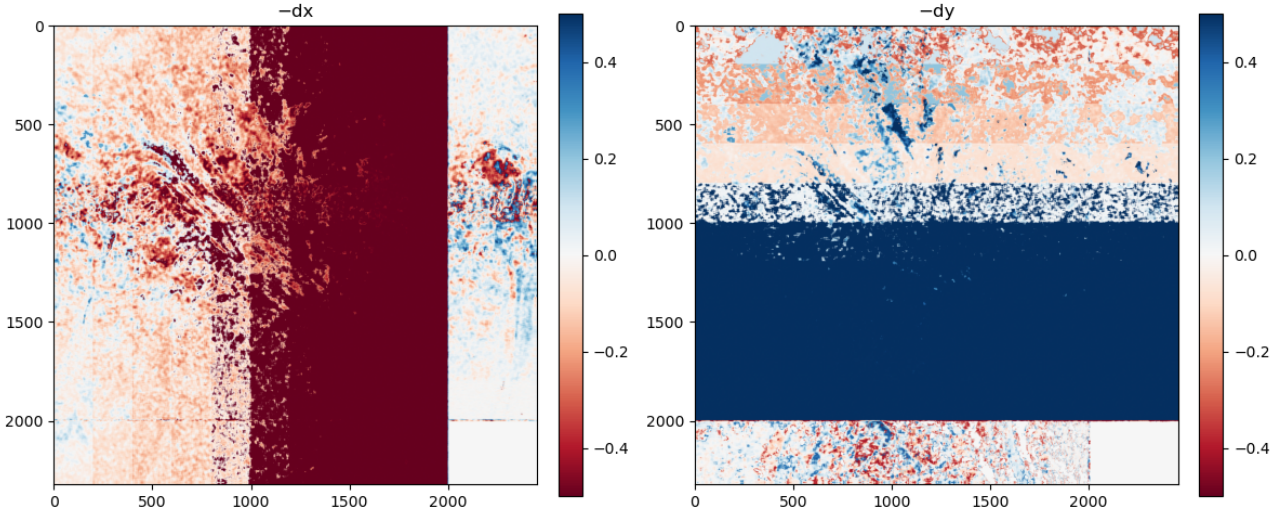

Figure S16. $\mathrm{NCC}_{\mathrm{FFT}}$ gaussian subpixel refinement residuals.

S2.2 PCC

PCC is a frequency-domain technique that estimates the translational offset between two image patches by analyzing the phase shift in their Fourier transforms. Unlike NCC, which uses both amplitude and phase, PCC relies exclusively on the phase information. PCC is computed as:

$$\mathrm{PCC}(u,v) = \mathcal{F}^{-1}\left(\frac{\mathcal{F}(R)\cdot\mathcal{F}(T)^{*}}{|\mathcal{F}(R)\cdot\mathcal{F}(T)^{*}|+\epsilon}\right) \tag{2}$$

The result of this expression is a correlation surface in the spatial domain, where the location of the global peak corresponds to the pixel-level displacement (u, v) between the two chips. PCC is particularly effective for subpixel registration when the images differ primarily by a rigid translation and are free from significant intensity or contrast differences.

Table S2. PCC subpixel refinement: bias, NMAD, and per-block runtimes

Method	Bias_x	Bias_y	NMAD_x	NMAD_y	Runtime per block (s)
center of mass	-0.03201	0.00186	0.14910	0.14505	5.66×10^{-5}
parabolic	-0.025998	0.00394	0.13612	0.18127	3.43×10^{-5}
gaussian	-0.11741	0.25613	0.51798	0.78255	5.31×10^{-5}
os3	-0.04198	0.00000	0.08257	0.14017	8.70×10^{-5}
os5	-0.13053	0.10131	0.16984	0.14511	9.97×10^{-5}
os7	-0.22563	0.20247	0.28562	0.23935	1.09×10^{-4}
ipg	-0.25038	0.26075	0.39110	0.39450	8.62×10^{-5}
ensemble	-0.15654	0.20281	0.24261	0.32055	2.29×10^{-4}

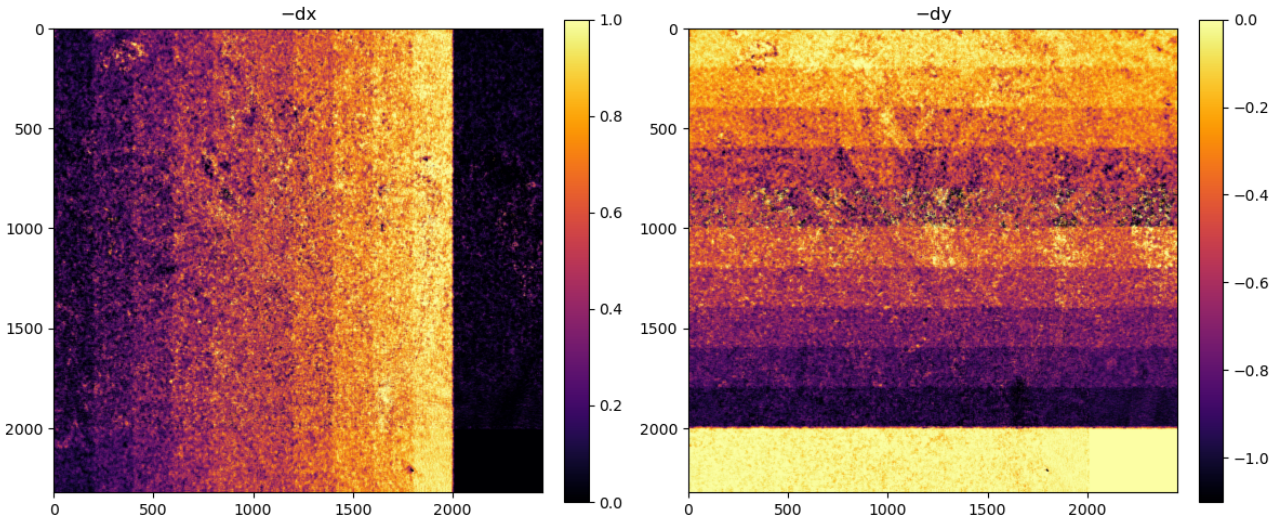

Figure S17. PCC center of mass subpixel refinement estimates.

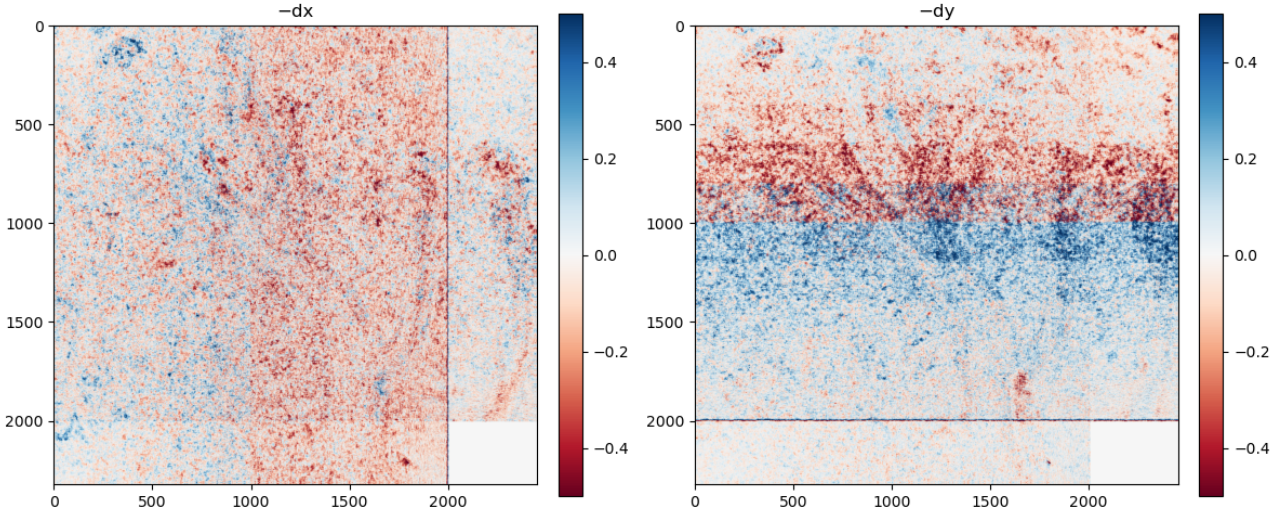

Figure S18. PCC center of mass subpixel refinement residuals.

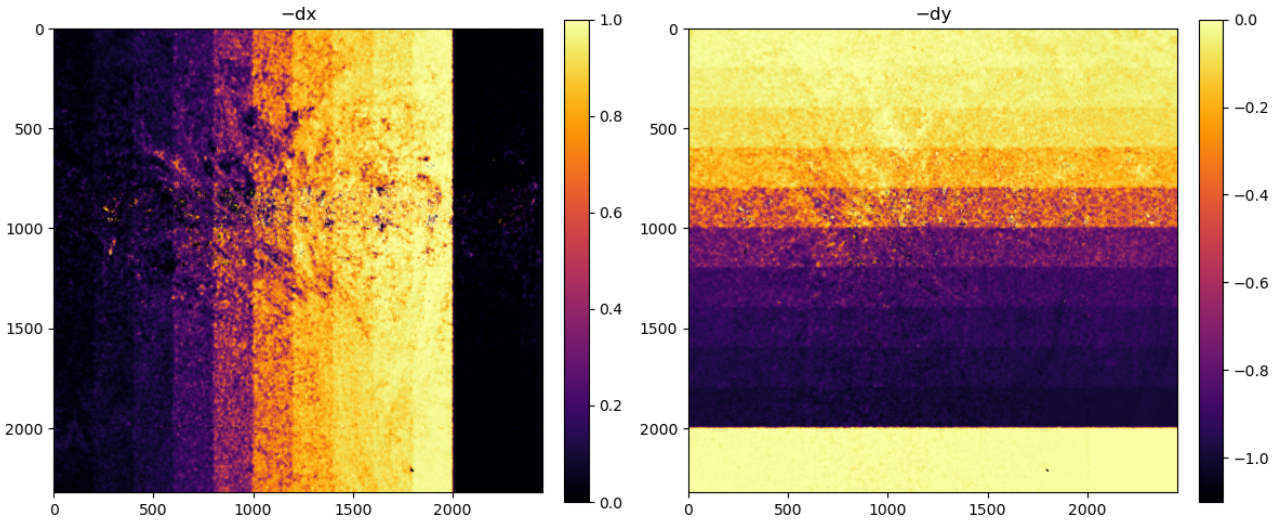

Figure S19. PCC parabolic subpixel refinement estimates.

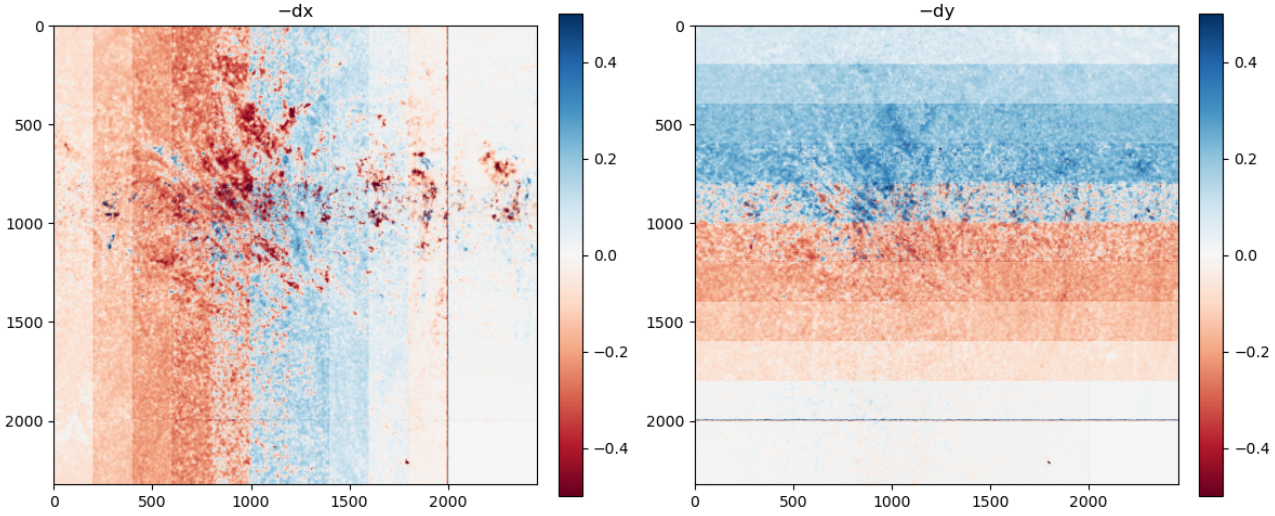

Figure S20. PCC parabolic subpixel refinement residuals.

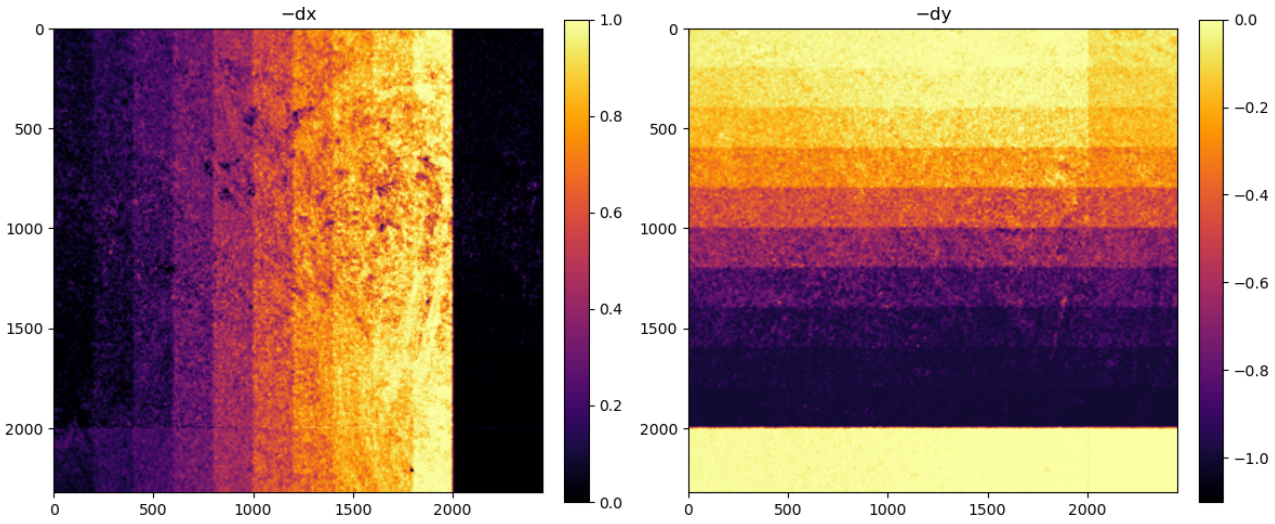

Figure S21. PCC os3 subpixel refinement estimates.

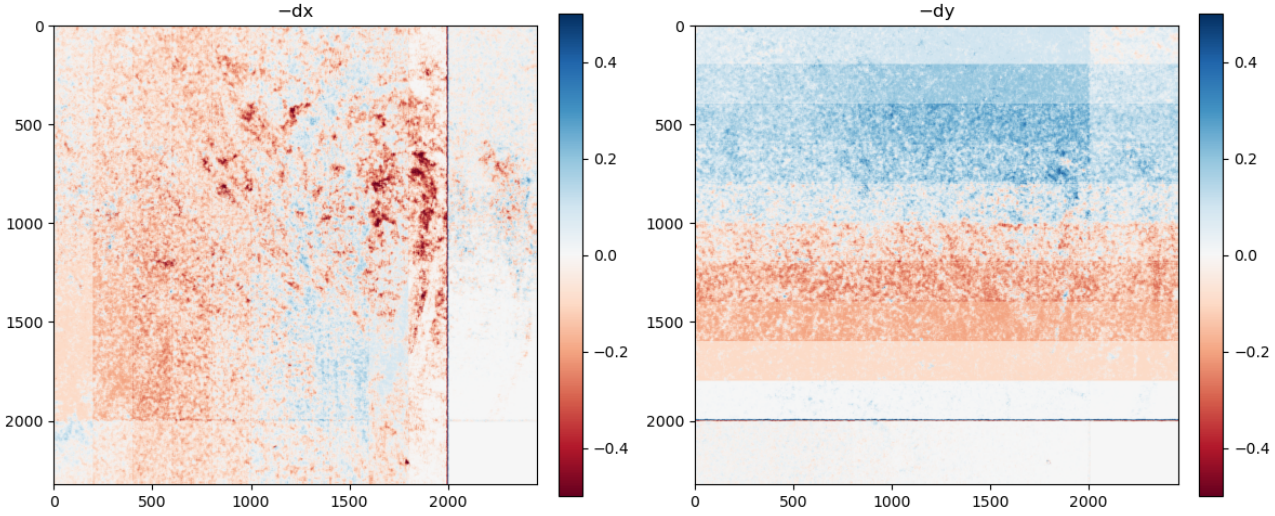

Figure S22. PCC os3 subpixel refinement residuals.

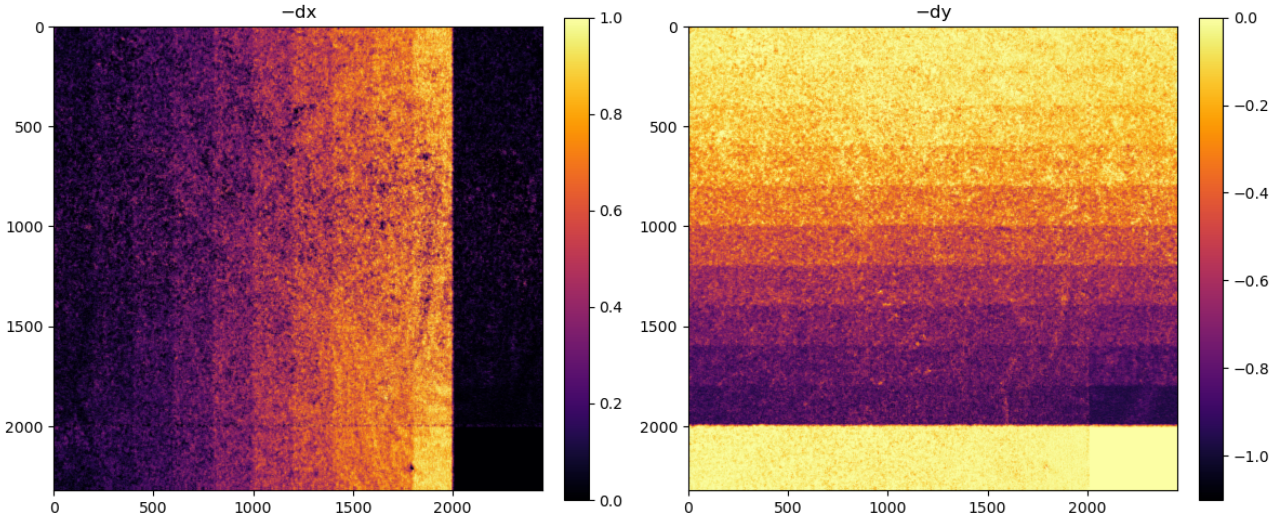

Figure S23. PCC os5 subpixel refinement estimates.

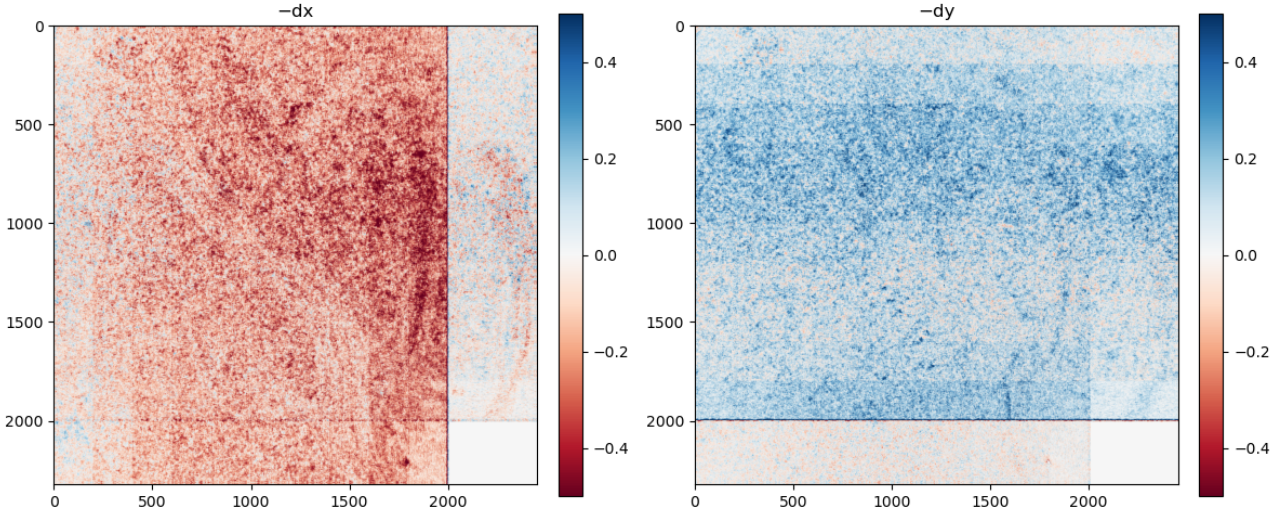

Figure S24. PCC os5 subpixel refinement residuals.

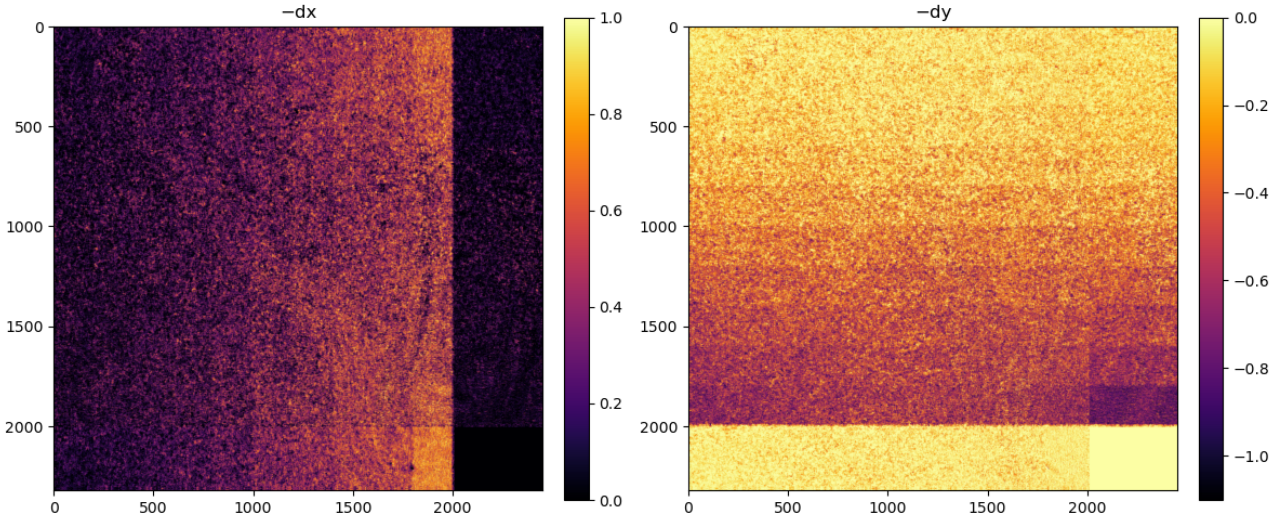

Figure S25. PCC os7 subpixel refinement estimates.

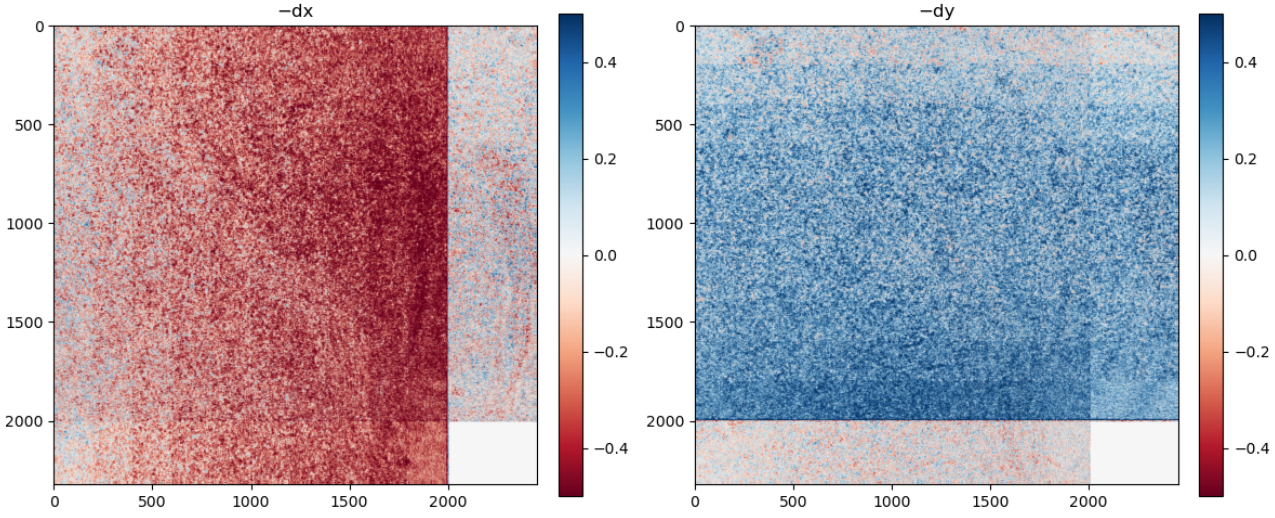

Figure S26. PCC os7 subpixel refinement residuals.

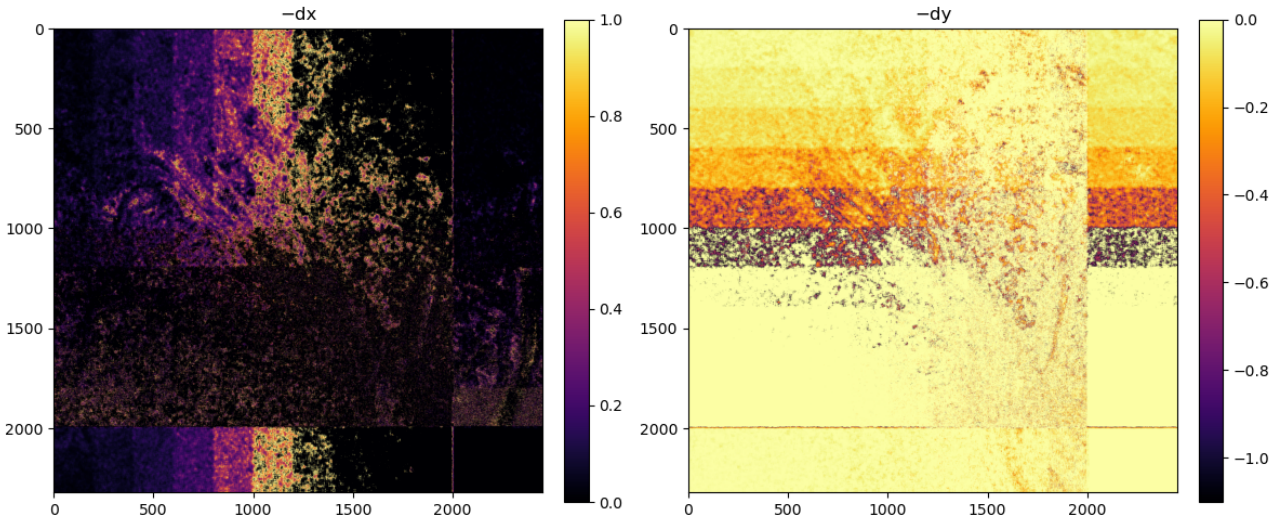

Figure S27. PCC ipg subpixel refinement estimates.

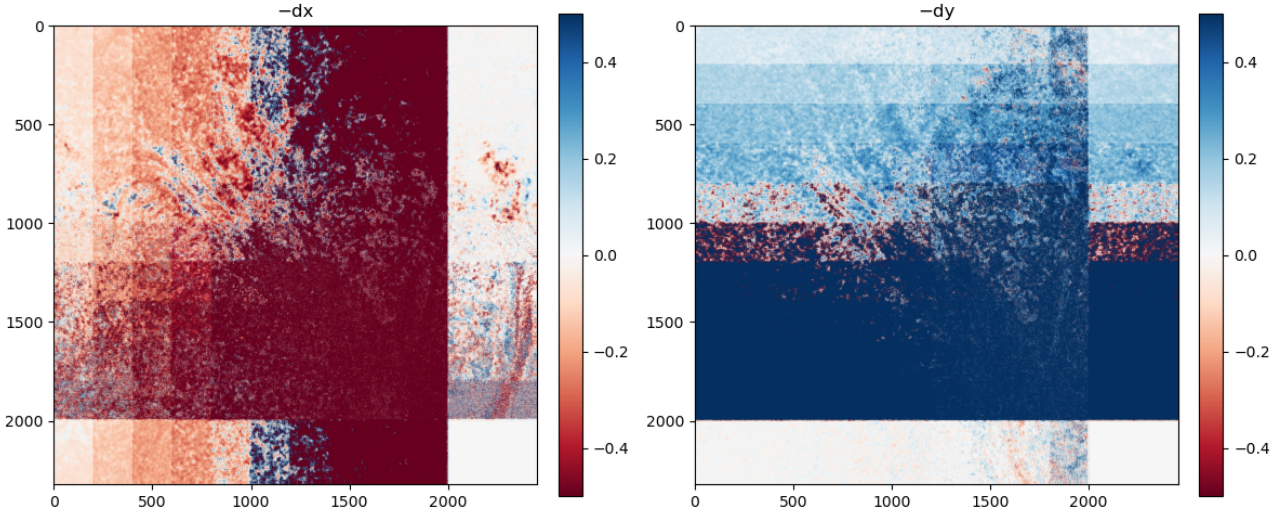

Figure S28. PCC ipg subpixel refinement residuals.

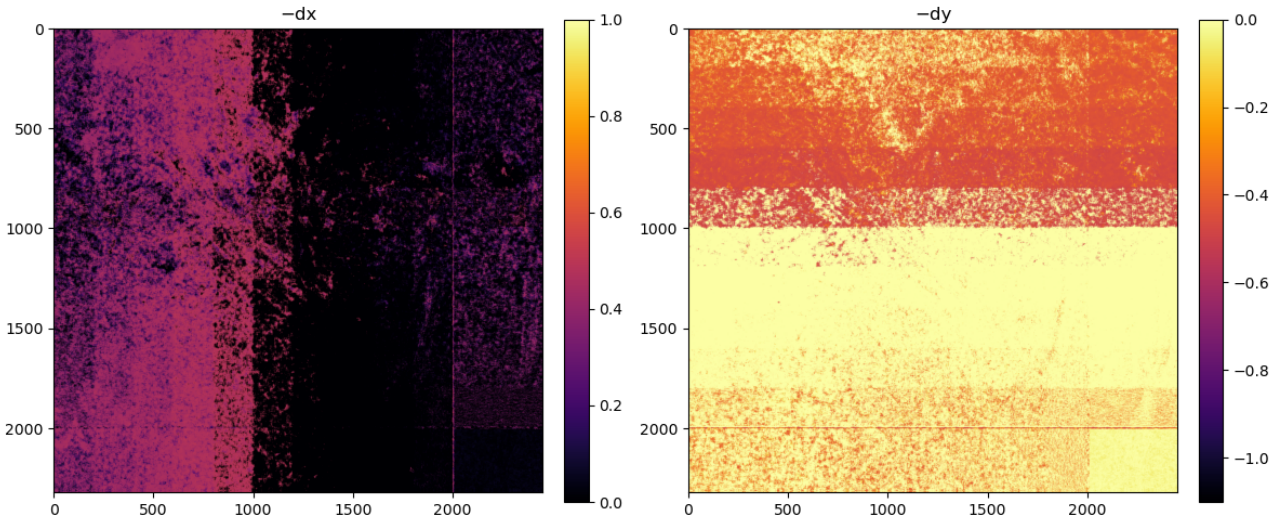

Figure S29. PCC gaussian subpixel refinement estimates.

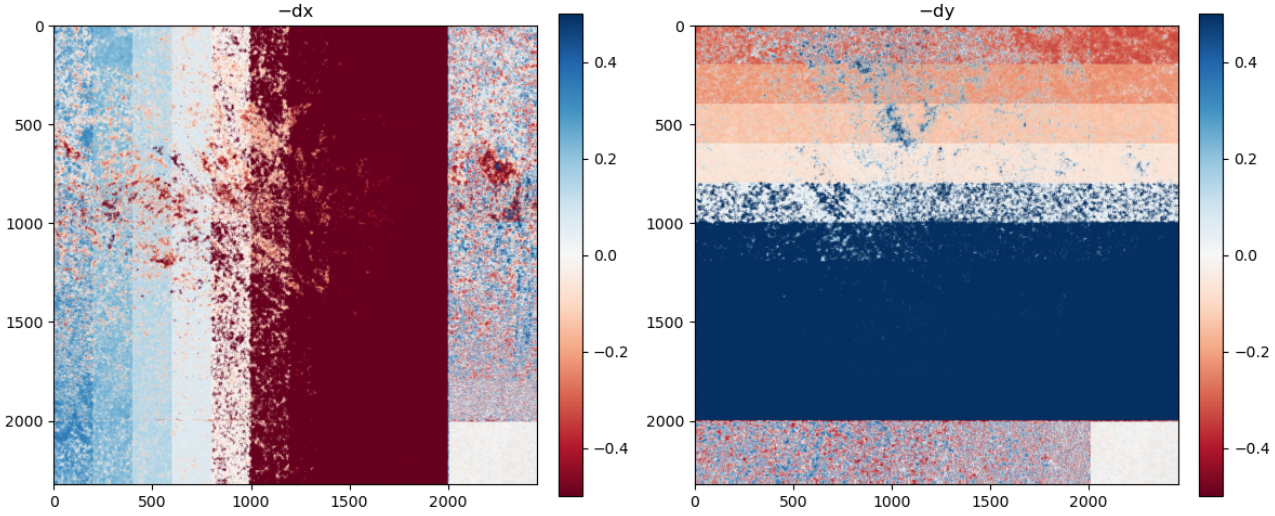

Figure S30. PCC gaussian subpixel refinement residuals.

References

Guizar-Sicairos, M., Thurman, S. T., and Fienup, J. R.: Efficient subpixel image registration algorithms, Optics letters, 33, 156–158, 2008.

Liu, G., Li, M., Zhang, W., and Gu, J.: Subpixel Matching Using Double-Precision Gradient-Based Method for Digital Image Correlation, Sensors, 21, https://doi.org/10.3390/s21093140, 2021.

Zheng, W., Bhushan, S., Van Wyk De Vries, M., Kochtitzky, W., Shean, D., Copland, L., Dow, C., Jones-Ivey, R., and Pérez, F.: GLAcier Feature Tracking testkit (GLAFT): a statistically and physically based framework for evaluating glacier velocity products derived from optical satellite image feature tracking, The Cryosphere, 17, 4063–4078, https://doi.org/10.5194/tc-17-4063-2023, 2023.